Bioorg. Med. Chem. Lett. 45 (2021) 128133

Contents lists available at ScienceDirect

Bioorganic & Medicinal Chemistry Letters

journal homepage: www.elsevier.com/locate/bmcl

Identification of aryl sulfonamides as novel and potent inhibitors of $Na_V1.5$

Shaoyi Sun *, Qi Jia, Alla Y. Zenova, Sophia Lin, Angela Hussainkhel, Janette Mezeyova, Elaine Chang, Samuel J. Goodchild, Zhiwei Xie, Andrea Lindgren, Gina de Boer, Rainbow Kwan, Kuldip Khakh, Luis Sojo, Paul Bichler, J.P. Johnson Jr., James R. Empfield, Charles J. Cohen, Christoph M. Dehnhardt, Richard Dean

Xenon Pharmaceuticals Inc., 200-3650 Gilmore Way, Burnaby, BC V5G 4W8, Canada

ARTICLE INFO

Keywords:
Aryl sulfonamide
$Na_V1.5$
Cardiac arrhythmia
LQT-3

ABSTRACT

We describe the synthesis and biological evaluation of a series of novel aryl sulfonamides that exhibit potent inhibition of $Na_V1.5$. Unlike local anesthetics that are currently used for treatment of Long QT Syndrome 3 (LQT-3), the most potent compound (-)-**6** in this series shows high selectivity over hERG and other cardiac ion channels and has a low brain to plasma ratio to minimize CNS side effects. Compound (-)-**6** is also effective in shortening prolonged action potential durations (APDs) in a pharmacological model of LQT-3 syndrome in pluripotent stem cell-derived cardiomyocytes (iPSC-CMs). Unlike most aryl sulfonamide Na_V inhibitors that bind to the channel voltage sensors, these $Na_V1.5$ inhibitors bind to the local anesthetic binding site in the central pore of the channel.

The cardiac voltage-gated sodium channel $Na_V1.5$ (*SCN5A* gene) is expressed mainly in the cell membrane of cardiomyocytes, including the sarcolemma of atrial and ventricular myocytes, Purkinje fibers, sino-atrial, and atrio-ventricular nodes.[1] The rapid upstroke of the cardiac action potential and the rapid impulse conduction through cardiac tissue is due to sodium influx via $Na_V1.5$ channels. Mutations in the *SCN5A* gene result in the genesis of a variety of cardiac arrhythmias. Hundreds of unique *SCN5A* mutations have been identified in patients, with the vast majority being in two primary inherited cardiomyopathies, either long QT syndrome type 3 (LQT-3, gain-of-function)[2–5] or Brugada syndrome (BrS, loss-of-function).[6] In addition, *SCN5A* mutations have also been reported in association with other cardiac disorders, including sick sinus syndrome,[7] atrial standstill,[8] cardiac conduction defect (CCD),[9] atrial fibrillation (AF),[10,11] and dilated cardiomyopathy (DCM).[12]

Sodium channel blocker therapy has been extensively used in treating cardiac arrhythmias, with many therapeutically useful anti-arrhythmic agents targeting $Na_V1.5$ (e.g. local anesthetics such as mexiletine **1**).[13] Although these drugs are widely used, they suffer from dose-limiting adverse effects, especially nausea and dizziness.[14] Ranolazine (**2**), structurally similar to other class I anti-arrhythmic agents, is currently marketed for the treatment of chronic angina. Although the mechanism of its antianginal effects is not known, **2** does inhibit $Na_V1.5$, and has significant anti-arrhythmic effects in both ventricles and atria. Unfortunately, **2** blocks **β**-adrenergic receptors, and inhibits a number of cardiac ion currents (e.g., human ether-à-go-go-related gene, hERG).[15,16] A more potent compound, GS-967 (**3**), was found to have high brain penetration and high activity on brain sodium channel isoforms (e.g., $Na_V1.1$, $Na_V1.2$, & $Na_V1.6$).[17] Eleclazine (**4**), purportedly selective over brain sodium channel isoforms, was discontinued from clinical development.[18]

In an effort to identify structurally distinct $Na_V1.5$ inhibitors with high selectivity over hERG and limited brain exposure, the corporate compound repository was surveyed. Aryl sulfonamide *rac*-**5** was found to be a modest $Na_V1.5$ inhibitor. We were intrigued by its structural feature because aryl sulfonamide is a well-known structure for subtype selective inhibitors of $Na_V1.7$ and, in general, displays low hERG activity and low central nervous system (CNS) penetration. Herein, we describe our efforts in the optimization of *rac*-**5** that led to the identification of a series of novel $Na_V1.5$ inhibitors including (-)-**6**, a potent $Na_V1.5$ inhibitor with high selectivity over hERG and other cardiac ion channels and low brain penetration.

The synthesis of these aryl sulfonamides is exemplified by *rac*-**6** as illustrated in Scheme 1, in general, via a S_NAr reaction joining a 3-substituted piperidin-4-ol left-hand fragment (LHF) with a suitably protected heteroaryl sulfonamide right-hand fragment (RHF) through an oxygen linkage. Construction of the LHF (*rac*-**11**) was commenced by

* Corresponding author.
E-mail address: ssun@xenon-pharma.com (S. Sun).

https://doi.org/10.1016/j.bmcl.2021.128133
Received 7 April 2021; Received in revised form 11 May 2021; Accepted 19 May 2021
Available online 24 May 2021

Suzuki-Miyaura cross-coupling reaction of vinylboronic acid pinacol ester **7** with 4-bromo-1,2-difluorobenzene to form **8**. Conversion of **8** to *rac*-**10** was initially carried out by hydroboration-oxidation method.[19] This method, however, only produced *rac*-**10** in 15% yield. Therefore, we investigated different approaches and found an efficient method for preparation of *rac*-**10**. To this end, we carried out an epoxidation of **8** using *m*-CPBA and subsequent hydrogenation of epoxide *rac*-**9** using molybdenum-promoted (1 wt%) nickel (skeletal) as the catalyst to provide *rac*-**10** in 56% yield over two steps. To our knowledge, this represents the first example of stereoselective preparation of a *trans* cyclic alcohol via metal-catalyzed reduction of an epoxide. In contrast, when Pd/C was used as the catalyst in this reaction, only the *cis*-isomer was isolated. With an efficient access to *rac*-**10** at hand, we were now in a position to complete the synthesis of the key intermediate *rac*-**11**. Treatment of *rac*-**10** with methanolic HCl, followed by alkylation with 2,2,2-trifluoroethyl trifluoromethanesulfonate under basic conditions provided intermediate *rac*-**11**. The RHF **15** was built by addition of aryl sulfonyl chloride **14** to the 2,4-dimethoxybenzyl (DMB) protected 2-amino 6-fluoropyridine intermediate **13**[20] in the presence of a base. Finally, NaH-mediated S_NAr reaction of *rac*-**11** and **15**, and subsequent TFA cleavage of the DMB protecting group of *rac*-**12** completed the synthesis of compound *rac*-**6**.

Taking *rac*-**5** as a starting point, our initial structure–activity relationship (SAR) studies focused on replacing the 1,2,4-thiadiazole moiety in *rac*-**5** to improve $Na_V1.5$ potency, and investigating different five- and six-membered nitrogen-containing heterocycles. This effort provided us several compounds with improved $hNa_V1.5$ activity relative to *rac*-**5**: the 4-thiazole *rac*-**17** (IC_{50} = 1.18 μM) and 6-fluoropyridine *rac*-**23** (IC_{50} = 0.70 μM) were revealed to be the two most potent $hNa_V1.5$ inhibitors. A brief SAR investigation on *rac*-**23** was executed; the results are shown in Table 1. Shifting the fluorine from the 6-position to the 3- or 5-position, as in *rac*-**24** and *rac*-**26**, resulted in a significant decrease in activity. However, 4-fluoropyridine analog *rac*-**25** maintained similar potency to *rac*-**23**. Replacing the 6-fluoropyridine in *rac*-**23** with 6-chloropyridine (*rac*-**27**) also maintained the inhibitory activity, while a significant decrease in potency was observed with 6-trifluoromethyl pyridine analog (*rac*-**28**).

Given its improved potency of $hNa_V1.5$ inhibition compared to *rac*-**5**, the pyridyl analogue *rac*-**23** was taken as an advanced lead for further optimization. Related SAR is summarized in Table 2. Incorporation of fluorine at either the 3- (*rac*-**30**) or 4-position (*rac*-**31**) of the left-hand phenyl ring resulted in only a small improvement in potency and metabolic stability, while 2-fluorine (*rac*-**29**) had no effect. Fluorination of both the 3- and 4- positions proved effective, as *rac*-**33** was about 2-fold more potent than *rac*-**23** and displayed improved metabolic stability. Polar substitutions on the left-hand phenyl ring were not tolerated, for example a nitrile group in *rac*-**34** resulted in a significant loss in $hNa_V1.5$ potency, while the complete lack of activity of the methylsulfonyl analog *rac*-**35** was quite striking.

Compound *rac*-**33** showed an attractive profile due to good $hNa_V1.5$ potency and *in vitro* microsomal stability. Therefore, we decided to study this compound further. The optically pure enantiomers were obtained by chiral separation and evaluated individually; however, the absolute stereochemistry could not be determined readily, and instead the first eluting enantiomer from the chiral column was assigned as (-)-**33** ($[\alpha]_D^{21}$ = -18.90, *c* 2.1, DMF) and the second eluting enantiomer was assigned as (+)-**33** ($[\alpha]_D^{21}$ = +18.74, *c* 2.1, DMF). (-)-**33** was slightly more potent with an IC_{50} value of 0.24 μM on $hNa_V1.5$.

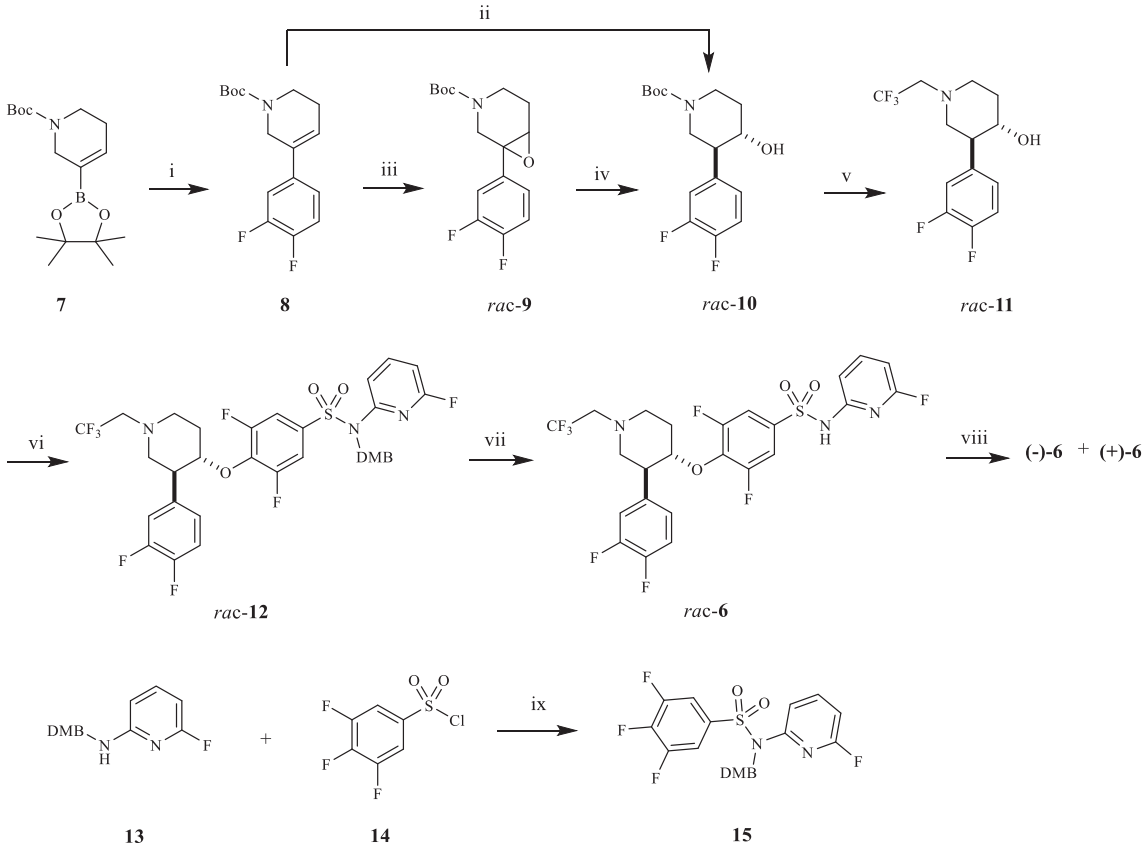

Scheme 1. Preparation and chiral separation of compound *rac*-**6**. Reagents and conditions: (i) 4-bromo-1,2-difluorobenzene, K_2CO_3, $Pd(PPh_3)_4$, 1,4-dioxane, H_2O, 90 °C, 18 h, 94%. (ii) BH_3·THF, THF, 0 °C to rt, 3 h then $NaBO_3$·$4H_2O$, 0 °C to rt, 16 h, 15%. (iii) *m*-CPBA, CH_2Cl_2, 0 °C to rt, 14 h, 82%. (iv) Molybdenum promoted (1 wt%) nickel (skeletal), methanol, 50 psi H_2, rt, 7 h, 69%. (v) 4 M HCl-MeOH, rt, 0.5 h; K_2CO_3, 2,2,2-trifluoroethyl trifluoromethanesulfonate, CH_3CN, rt, 14 h, 82%. (vi) **15**, NaH, DMF, 0 °C to rt, 18 h. (vii) TFA, CH_2Cl_2, 0 °C to rt, 1 h, 60% in 2 steps. (viii) Chiral SFC. (ix) MeLi, THF, −78 °C to rt, 15 min., then **14**, −78 °C to rt 1.5 h, 84%.

Table 1
$Na_V1.5$ activity of compounds *rac*-**5**, and *rac*-**16** – *rac*-**28**.

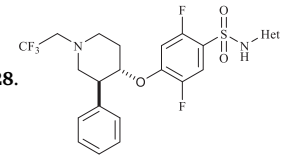

Compd[a]	Het	$hNa_V1.5$ IC_{50} (μM) [b]	Compd[a]	Het	$hNa_V1.5$ IC_{50} (μM) [b]
rac-**5**		7.83	*rac*-**16**		25.05
rac-**17**		1.18	*rac*-**18**		4.65
rac-**19**		7.14	*rac*-**20**		>30
rac-**21**		25.49	*rac*-**22**		4.32
rac-**23**		0.70	*rac*-**24**		5.04
rac-**25**		1.29	*rac*-**26**	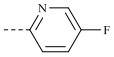	13.21
rac-**27**	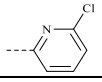	1.10	*rac*-**28**	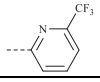	6.33

[a] All compounds exhibited spectral data consistent with their proposed structures and had analytical purities >94% as determined by HPLC.
[b] IC_{50}s were an average of at least two independent determinations using automated voltage clamp electrophysiology.

We subsequently discovered analog *rac*-**6**, which was about 4-fold more potent than *rac*-**33**. However, this improvement came at the cost of lower microsomal stability. We postulated that the increased metabolic clearance of *rac*-**6** might be due to the absence of the 2-fluoro substituent of the central phenyl ring; disappointingly, addition of a 2-fluorine in *rac*-**36** did not lead to improvement in metabolic stability. Furthermore, replacement of the central phenyl ring with a pyridyl ring, compound *rac*-**37**, displayed similar metabolic stability as *rac*-**33**, but with erosion of $hNa_V1.5$ activity. For comparison, the 4-thiazole analog *rac*-**38** was also prepared and found to be not as efficient as its 6-fluoropyridine counterpart *rac*-**33** in $Na_V1.5$ inhibition and metabolic stability, consistent with the earlier SAR.

Chiral separation of *rac*-**6** provided two optically pure enantiomers (-)-**6** ($[\alpha]_D^{21}$ = -7.95, *c* 2.1, DMF) and (+)-**6** ($[\alpha]_D^{21}$ = +7.52, *c* 2.1, DMF). (-)-**6** was about 4-fold more potent than (+)-**6** with an IC_{50} value of 0.039 μM on $hNa_V1.5$. Further evaluation of (-)-**6** suggested that (-)-**6** had 16-, 7-, and 6-fold selectivity over CNS sodium channel isoforms $hNa_V1.1$, 1.2, and 1.6 (IC_{50}s of 0.62, 0.27, and 0.23 μM, respectively.), when measured by whole cell voltage clamp (EP). The EP protocol used to optimize potency on $Na_V1.5$ was designed to maximize interaction with the high affinity state of the channel and best approximate the K_d for binding to $Na_V1.5$, especially for potent compounds that have slow kinetics of binding equilibration. We have found that using this protocol for selectivity assessments can overestimate the true selectivity of compounds that have differentiated rates of equilibrium with distinct channel isoforms. For this reason, we also measured compound isoform selectivity with a different ($V_{½}$) protocol that we believe better assesses the physiologically relevant selectivity. In this selectivity protocol, potency (IC_{50}) on $hNa_V1.5$, 1.1, 1.2, 1.6 changed to 0.11, 0.09, 0.012, and 0.11 μM, respectively, suggesting that the apparent selectivity seen in the SAR protocol is not likely to translate to an *in vivo* setting.

Compound (-)-**6** was also evaluated in a sodium influx assay[21] for its inhibitory activities on $hNa_V1.5$, 1.1, 1.2, 1.6 and 1.7, and exhibited IC_{50} values of 0.044, 0.56, 0.27, 0.11, and 0.22 μM, respectively.

Table 2
$Na_V1.5$ activity and metabolic stability of compounds *rac*-**23**, and *rac*-**29** – *rac*-**38**.

Compound[a]	Ar	X	Y	HET	$hNa_V1.5$ IC_{50} (μM) [b]	HLM, MLM CL_{hep} (mL/min/kg)
rac-**23**		C (F)	C (H)		0.70	16, 70
rac-**29**		C (F)	C (H)		0.68	17, 71
rac-**30**		C (F)	C (H)		0.46	13, 53
rac-**31**	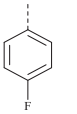	C (F)	C (H)		0.61	11, 62
rac-**32**		C (F)	C (H)		0.47	13, 49
rac-**33**		C (F)	C (H)		0.26	7.5, 49
(-)–**33**	enantiomer 1				0.24	9.0, 50
(+)–**33**	enantiomer 2				0.43	7.0, 45
rac-**34**		C (F)	C (H)		4.58	nd[c]
rac-**35**		C (F)	C (H)		>30	nd[c]
rac-**6**		C (H)	C (F)		0.065	15, 65
(-)-**6**	enantiomer 1				0.039	13, 63
(+)-**6**	enantiomer 2				0.17	14, 74
rac-**36**		C (F)	C (F)		0.031	14, 65
rac-**37**		C (H)	N		1.55	8.4, 63
rac-**38**	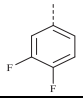	C (F)	C (H)		0.75	14, 70

[a] All compounds exhibited spectral data consistent with their proposed structures and had analytical purities >94% as determined by HPLC.
[b] IC_{50}s were an average of at least two independent determinations using automated voltage clamp electrophysiology.
[c] nd: not determined.

Compounds (-)-**33** and (-)-**6** were found to have negligible inhibition on CYPs 1A2, 3A4, 2C19, 2D6, and moderate inhibition on CYP2C9 (IC_{50}s of 6.9, and 2.2 μM for (-)-**33** and (-)-**6**, respectively.). Importantly, (-)-**6** was highly selective, when tested by voltage clamp against a panel of heterologously expressed cardiac ion channels including hERG, $K_V2.1$, $K_V1.5$, $K_V3.2$, HCN2, HCN4, $K_V4.2$KChIP2.2, $K_V4.3$KChIP2.2,

K_VLQT1/mink, Ca_V1.2, Ca_V2.2, Ca_V3.1, Ca_V3.3, GABA, TRPV1, and 5-HT3A. For example, **(-)-6** showed 5% inhibition on hERG at 10 μM concentration.

The pharmacokinetic (PK) properties of (-)–**33** and **(-)-6** were determined in mouse (Table 3). Consistent with the predicted CL_{hep} and high plasma protein binding (99.8% bound), both compounds exhibited low plasma clearance (CL), moderate terminal half-lives ($t_{½}$) and low volume of distribution (V_{ss}). The oral bioavailability of (-)–**33** and **(-)-6** were 45%, and 39%, respectively. In addition, both (-)–**33** and **(-)-6** exhibited low brain levels, suggesting that the activity on CNS sodium channel isoforms was not a concern.

Next, we evaluated the activity of **(-)-6** in shortening prolonged action potential durations (APDs) like those often observed in long QT syndrome-3 (LQT-3) patients carrying gain-of-function *SCN5A* mutations. The *Anemonia sulcata* toxin II (ATX-II) is known to slow the inactivation of $Na_V1.5$[22], thereby increasing total sodium flux and simulating a gain-of-function *SCN5A* mutation that causes a persistent sodium current, which would lead to a prolongation of the APD. In this study we used an ATX-II-induced model of prolonged APD in human induced pluripotent stem cell cardiomyocytes (iPSC-CMs) utilizing current clamp to record the APD of spontaneously beating iPSC-CMs. Only cells with maximum diastolic potentials < -75 mV and ventricular-like AP morphology (upstroke velocity > 70 V/s) were used. With the addition of 15–30 nM ATX-II, prolongation of the APD was observed in the iPSC-CMs with a 25–100% increase in APD_{90}, depending on the sensitivity of the cell (Fig. 2). Addition of 100 nM **(-)-6** (2.5 × $Na_V1.5$ IC_{50}) concurrently with ATX-II shortened the ATX-II-induced prolongation by 84%, returning it close to vehicle. Compound **(-)-6** showed no effect on AP amplitude or maximum diastolic membrane potential (Fig. S2A in supplementary data), however, it did cause a small reduction in upstroke velocity dV/dt(Vmax) of 23% (Fig. S2B in supplementary data).

It has been reported that mexiletine (**1**), ranolazine (**2**), GS-967 (**3**) and eleclazine (**4**) inhibit the $Na_V1.5$ late (persistent) current (I_{Na}) (Fig. 1), which is enhanced in LQT3 patients and other cardiac pathological conditions, such as ischemic heart disease.[13,17,18] By blocking the late sodium current during ischemia, these drugs inhibit the subsequent sodium-calcium overload within the myocyte that is normally a hallmark of an ischemic cell.[23] We therefore determined the selectivity of **(-)-6** for inhibiting the $Na_V1.5$ late I_{Na} over the $Na_V1.5$ peak I_{Na}. Analogous to the iPSC experiment, ATX-II was used to generate $Na_V1.5$ late I_{Na} in HEK cells stably expressing $hNa_V1.5$ and both peak and late $Na_V1.5$ currents were measured at a holding potential of −95 mV, similar to the resting membrane potential of the iPSC cardiomyocytes. Unfortunately, the ratio of IC_{50} values for inhibition of peak and late I_{Na} by **(-)-6** was only 1.1-fold (peak/late IC_{50} 17.7/15.8 nM). This suggests that in the ATX-II-induced iPSC model at least, it appears that the efficacy is mainly driven by total $Na_V1.5$ inhibition at the resting membrane potential of a cardiomyocyte, rather than selective block of late I_{Na} as **(-)-6** had a reduction in prolonged APD yet no peak/late selectivity.

Table 3
PK profiles of compounds (-)–**33** and **(-)-6**[a].

Compound	(-)–**33**	**(-)-6**
iv		
CL (mL/min/kg)	1.8	3.8
$t_{½}$ (h)	4.3	2.6
V_{ss} (L/Kg)	0.6	0.8
AUC (μM.h)	16	7.6
po		
C_{max} (μM)	5.2	3.6
$t_{½}$ (h)	4.1	2.7
AUC (μM.h)	72	30
F (%)	45	39
C_b/C_p @ 2 h (μM) (ratio)	2.62/9.37 (0.28)	2.03/6.44 (0.32)

[a] Average of 3 male FVB mice. Intravenous dosed with 1 mg/kg of compound (-)–**33** or **(-)-6** in PEG400 and 50% 2-Hydroxypropyl-β-cyclodextrin in saline (40:60). Orally dosed with 10 mg/kg of compound (-)–**33** or **(-)-6** as a suspension in 0.5% w/w methyl cellulose and 0.2% v/v tween 80 in water.

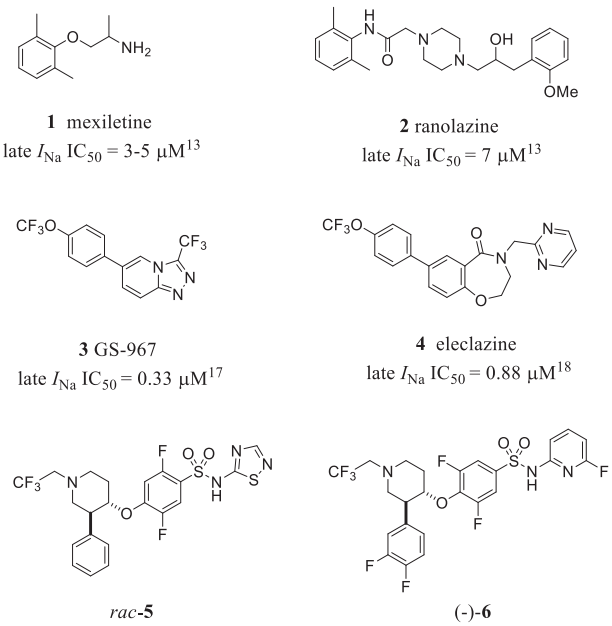

Fig. 1. Selected $Na_V1.5$ inhibitors and compounds *rac*-**5** and **(-)-6**.

To investigate the binding mode of $Na_V1.5$ inhibition, we performed mutagenesis studies using compounds *rac*-**17** and *rac*- **23** (Table 4). Recently, subtype-selective aryl sulfonamide Na_V inhibitors with an anionic warhead have been shown to bind to a positively charged gating residue, the fourth Arg in segment S4 (R4) in the $Na_V1.7$ voltage sensor of domain IV (VSD4).[24,25] Therefore, we evaluated the binding of compounds *rac*-**17** and *rac*-**23** on the equivalent VSD4 R1631A (R4A) mutation in $Na_V1.5$ using the VSD4 blocker GX-4195[25] as a control. This mutant led to more than 18-fold decrease in $Na_V1.5$ potency for GX-4195, however, no clear potency drop was observed for *rac*-**17** or *rac*-**23**, suggesting that *rac*-**17** and *rac*-**23** do not have interactions with the positively charged gating residue (R4) in VSD4. Furthermore, *rac*-**23** was also evaluated on VSD4 R1622A (R1A), R1625A (R2A), R1628A (R3A) and R1634A (R5A) mutants to determine if it engaged any of the other highly conserved arginines in VSD4. Again, no clear potency change was observed (IC_{50}s of 1.29, 0.81, 0.82 and 1.21 μM, respectively). We next hypothesized that this class of compounds might be binding to a corresponding conserved arginine in VSD2 instead of R4 in VSD4, thereby imparting its inhibitory activity through VSD2, similar to the peptide toxin ProTx-II.[26] We evaluated *rac*-**23** on a VSD2 R814A (R3A) mutant, which corresponds to R4 in VSD4, but saw no clear impact of the mutation (IC_{50} of 0.41 μM).

We continued to investigate the binding site for this class of compounds by site directed mutagenesis of phenylalanine 1759 to alanine (F1759A) in the pore domain of the $Na_V1.5$ channel followed by functional analysis. This residue, found in VSD4-S6, is known to be essential for binding of some antiarrhythmic agents, such as ranolazine,[27] in addition to the local anesthetics (e.g., lidocaine).[28] The potency of (-)–**33** for the mutated channel was reduced by>40-fold (IC_{50} > 10 μM), suggesting that these aryl sulfonamide $Na_V1.5$ inhibitors bind to the local anesthetic binding site in the pore domain.

We further tested the ability of compounds (-)–**33** and **(-)-6** to displace the [^{3}H]BNZA ligand. This ligand has been shown to bind to the pore of $Na_V1.5$ and most clinical local anesthetics inhibit binding of [^{3}H]BNZA.[29] This was also the case for (-)–**33** and **(-)-6** with K_i values of 2.02 and 0.37 μM, respectively. Furthermore, in voltage clamp studies of $Na_V1.5$ expressed heterologously in HEK cells, the state-dependence of block for **(-)-6**, was only 24-fold when comparing the shift in IC_{50} at

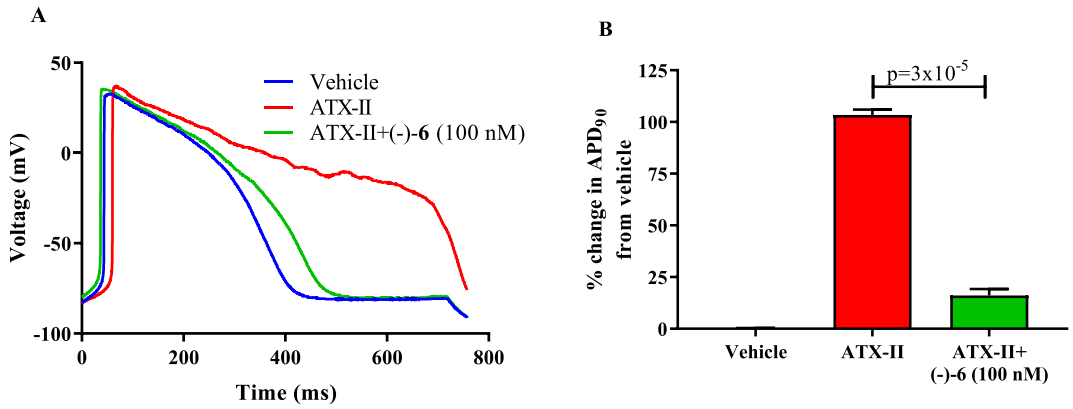

Fig. 2. Reversal of ATX-II-induced APD_{90} by 100 nM (-)-**6** in human iPSC-CM. Statistical significance of results were analyzed by T-test using Prism version 7 (GraphPad Software).

Table 4
Mutagenesis studies of *rac*-**17**, *rac*-**23** and GX-4195.

Compound	$hNa_V1.5$ IC_{50} (μM)	$hNa_V1.5$ VSD4 R4A IC_{50} (μM)
rac-**17**	1.18	1.17
rac-**23**	0.70	0.57
GX-4195	0.55	> 10

rested state (-120 mV) to a partially inactivated state (-95 mV) (Fig. S1 in supplementary data). This fold change is similar to lidocaine (35-fold), a pore-binding local anesthetic, but much smaller than a VSD4 binding sodium channel inhibitor such as GX-674 (2400-fold),[25] further supporting our conclusion that these aryl sulfonamides bind to the pore domain.

In summary, we have described the discovery of a series of novel aryl sulfonamide $Na_V1.5$ inhibitors. Mutagenesis studies suggest that these potent $Na_V1.5$ inhibitors bind to the local anesthetic binding site in the pore domain. The tool compound (-)-**6** is a potent $Na_V1.5$ inhibitor with significant advantages over currently available class I antiarrhythmic agents including its high selectivity over hERG and other cardiac ion channels, as well as its low brain penetration. Nonetheless, (-)-**6** is effective in shortening prolonged APDs induced by ATX-II in human iPSC-CMs. (-)-**6** represents a new probe in the research of the pharmacological functions on $Na_V1.5$.

The molybdenum-promoted (1 wt%) nickel (skeletal) catalyzed reduction of epoxides method provides a valuable synthetic entry to *trans* cyclic alcohols. Although the mechanism of the *trans* stereochemistry from this reduction is not known, this catalyst appears to be essential for this transformation. Potentially, enantioselective epoxidation of olefin **8** could be realized using Jacobsen's salen-type catalyst,[30] leading to the asymmetric synthesis of enantiomer (-)-**6** or (+)-**6** that could be assigned according to its optical rotation or its biological activities, thereby the absolute stereochemistry of (-)-**6** could be determined.

Declaration of Competing Interest

The authors declare that they have no known competing financial interests or personal relationships that could have appeared to influence the work reported in this paper.

Acknowledgements

The authors thank chemists at WuXi AppTec for their assistance in preparation of compounds *rac*-**18**-*rac*-**21**, *rac*-**27**, *rac*-**28** and *rac*-**34**, *rac*-**35**, as well as chiral separation of compounds *rac*-**33** and *rac*-**6**. The authors also thank Charles Rivers Laboratories for profiling the selectivity of compound (-)-**6** and in particularly Carlos Obejero-Paz for the evaluation of (-)-**6** in human iPSC-CMs. In addition, the authors thank Dr. Steven S. Wesolowski, as well as Professor Hiroyuki Kagechika and the reviewers for their suggestions during preparation and revision of this manuscript.

Appendix A. Supplementary data

Preparation and chiral separation of compound *rac*-**6**; ^1H NMR spectra of *rac*-**10** and its *cis*-isomer; protocols for $Na_V1.5$ *in vitro* profiling and efficacy assessment protocol in human iPSC-CMs. Supplementary data to this article can be found online at https://doi.org/10.1016/j.bmcl.2021.128133.

References

1 Amin AS, Asghari-Roodsari A, Tan HL. Cardiac sodium channelopathies. *Pflugers Arch.* 2010;460:223–237.
2 Wang Q, Shen J, Splawski I, et al. *SCN5A* mutations associated with an inherited cardiac arrhythmia long QT syndrome. *Cell.* 1995;80:805–811.
3 Bennett PB, Yazawa K, Makita N, George AL. Molecular mechanism for an inherited cardiac arrhythmia. *Nature.* 1995;376:683–685.
4 Goldenberg I, Moss AJ. Long QT syndrome. *J Am Coll Cardiol.* 2008;51:2291–2300.
5 Bokil NJ, Baisden JM, Radford DJ, Summers KM. Molecular genetics of long QT syndrome. *Mol Genet Metab.* 2010;101:1–8.
6 Hedley PL, JÄ¸rgensen P, Schlamowitz S, et al. The genetic basis of Brugada syndrome: a mutation update. *Hum Mutat.* 2009;30:1256–1266.
7 Benson DW, Wang DW, Dyment M, et al. Congenital sick sinus syndrome caused by recessive mutations in the cardiac sodium channel gene (*SCN5A*). *J Clin Invest.* 2003;112:1019–1028.
8 Groenewegen WA, Firouzi M, Bezzina CR, et al. A cardiac sodium channel mutation cosegregates with a rare connexin40 genotype in familial atrial standstill. *Circ Res.* 2003;92:14–22.
9 Schott J-J, Alshinawi C, Kyndt F, et al. Cardiac conduction defects associate with mutations in *SCN5A*. *Nat Genet.* 1999;23:20–21.
10 Olson TM, Michels VV, Ballew JD, et al. Sodium channel mutations and susceptibility to heart failure and atrial fibrillation. *JAMA.* 2005;293:447–454.
11 Ellinor PT, Nam EG, Shea MA, Milan DJ, Ruskin JN, MacRae CA. Cardiac sodium channel mutation in atrial fibrillation. *Heart Rhythm.* 2008;5:99–105.
12 Bezzina CR, Remme CA. Dilated cardiomyopathy due to sodium channel dysfunction, what is the connection? *Circ Arrhythm Electrophysiol.* 2008;1:80–82.
13 Antzelevitch C, Nesterenko V, Shryock JC, et al. The role of late I_{Na} in development of cardiac arrhythmias. *Handb Exp Pharmacol.* 2014;221:137–168.
14 Fenster PE, Comess KA. Pharmacology and clinical use of mexiletine. *Pharmacotherapy.* 1986;6:1–9.
15 Antzelevitch C, Belardinelli L, Zygmunt AC, et al. Electrophysiologic effects of ranolazine: a novel anti-anginal agent with antiarrhythmic properties. *Circulation.* 2004;110:904–910.
16 Antzelevitch C, Burashnikov A, Sicouri S, Belardinelli L. Electrophysiological basis for the antiarrhythmic actions of ranolazine. *Heart Rhythm.* 2011;8:1281–1290.
17 Koltun DO, Parkhill EQ, Elzein E, et al. Discovery of triazolopyridine GS-458967, a late sodium current inhibitor (late I_{Na}i) of the cardiac $Na_V1.5$ channel with improved efficacy and potency relative to ranolazine. *Bioorg Med Chem Lett.* 2016;26:3202–3206.
18 Zablocki JA, Elzein E, Li X, et al. Discovery of dihydrobenzoxazepinone (GS-6615) late sodium current inhibitor (late I_{Na}i), a phase II agent with demonstrated

preclinical anti-Ischemic and antiarrhythmic properties. *J Med Chem*. 2016;59:9005–9017.

19 The hydroboration-oxidation method worked well for unsubstituted phenyl substrate tert-butyl 5-phenyl-3,6-dihydropyridine-1(2H)-carboxylate and provided tert-butyl trans-4-hydroxy-3-phenylpiperidine-1-carboxylate in 51% yield, which was used in the synthesis of analogs rac-5 – rac-28.

20 Pero JE, Lehman HDGF, Kelly MJ III, et al. Benzoxazolinone compounds with selective activity in voltage-gated sodium channels. PCT Int. Appl. WO 2014066490 A1, May 1, 2014.

21 Safina BS, McKerrall SJ, Sun S, et al. Discovery of acyl-sulfonamide Nav1.7 Inhibitors GDC-0276 and GDC-0310. *J Med Chem*. 2021;64:2593–2966.

22 van Veen TAB, Stein M, Royer A, et al. Impaired impulse propagation in *Scn5a*-knockout mice: combined contribution of excitability, connexin expression, and tissue architecture in relation to aging. *Circulation*. 2005;112(13):1927–1935.

23 Belardinelli L, Shryock J C, Fraser H. Inhibition of the late sodium current as a potential cardioprotective principle: effects of the late sodium current inhibitor ranolazine. Heart. 2006;92(Suppl IV):iv6–iv14.

24 McCormack K, Santos S, Chapman ML, et al. Voltage sensor interaction site for selective small molecule inhibitors of voltage-gated sodium channels. *Proc Natl Acad Sci USA*. 2013;110:E2724–E2732.

25 Ahuja S, Mukund S, Deng L, et al. Structural basis of NaV1.7 inhibition by an isoform-selective small-molecule antagonist. Science. 2015;350:aac5464.

26 Sokolov S, Kraus RL, Scheuer T, Catterall WA. Inhibition of sodium channel gating by trapping the domain II voltage sensor with protoxin II. *Mol Pharmacol*. 2008;73(3):1020–1028.

27 Fredj S, Sampson KJ, Liu H, Kass RS. Molecular basis of ranolazine block of LQT-3 mutant sodium channels: evidence for site of action. *Br J Pharmacol*. 2006;148:16–24.

28 Mike A, Lukacs P. The enigmatic drug binding site for sodium channel inhibitors. *Curr Mol Pharm*. 2010;3(3):129–144.

29 Williams BS, Felix JP, Priest BT, et al. Characterization of a new class of potent inhibitors of the voltage-gated sodium channel $Na_V1.7$. *Biochemistry*. 2007;46(50):14693–14703.

30 McGarrigle EM, Gilheany DG. Chromium- and Manganese-salen promoted epoxidation of alkenes. *Chem Rev*. 2005;105(5):1563–1602.